



Original Research

## Abstraction of phenol onto *Pseudomonas putida* and Cetyl Trimethyl Ammonium Bromide

N. Saravani<sup>1</sup>, M. Arulmozhi<sup>1,\*</sup>, A. Anbuthangam<sup>2</sup>, M. Manimozhi<sup>3</sup>

<sup>1</sup> Bioprocess research laboratory, Department of Petrochemical Technology, Anna University, BIT Campus, Tiruchirappalli, India

<sup>2</sup> Department of Biotechnology and Genetic Engineering, Bharathidasan University, Tiruchirappalli, India

<sup>3</sup> School of Electrical Engineering, VIT University, Vellore, India

Correspondence to: [arulmozhisenthikumar@gmail.com](mailto:arulmozhisenthikumar@gmail.com)

Received March 17, 2016; Accepted May 15, 2017; Published July 31, 2017

Doi: <http://dx.doi.org/10.14715/cmb/2017.63.6.7>

Copyright: © 2017 by the C.M.B. Association. All rights reserved.

**Abstract:** Foam separation, an efficient downstream processing unit operation, was tested as a post-treatment technique for phenol removal after biosorption. The biosorptive foam separation process was carried out in two stages, namely biosorption and foam separation. A minimum run resolution V central composite design with four variables (initial concentration, pH, biosorbent dosage, and time) for biosorption and three variables (liquid pool height, surfactant concentration, and air flow rate) for biosorptive foam separation was applied to optimize the process. The results showed a good fit with the proposed statistical model for removal of phenol ( $R^2 = 0.9500$ ) for biosorption and ( $R^2 = 0.9599$ ) for biosorptive foam separation. In addition, the adsorption isotherm and kinetic studies revealed that the biosorption process followed the Langmuir model ( $R^2 = 0.9544$ ) and Bangham kinetic model ( $R^2 = 0.9857$ ). The adsorbed chemical species was identified by FTIR spectroscopy. Electrokinetic measurements were carried out to determine the isoelectric point (IEP) of the bacteria. The zeta potential profile of the bacteria appears to be negative throughout the range of pH examined, showing isoelectric point at a pH of 3. The recovery of phenol loaded biomass and final traces of phenol by flotation were found to be 99.95%.

**Key words:** Biosorptive foam separation; *Pseudomonas putida*; Cetyl Trimethyl Ammonium Bromide; Bangham kinetic model; Zeta potential.

### Introduction

The chemical surroundings consist of four million famous chemicals and a very large number of strange chemicals (1). Phenol is an important pollutant found in a variety of effluent streams from chemical industries such as resin, coke oven in steel plants, petrochemical, fertilizer plant, pharmaceuticals, chemical, dye industries, plastics, textiles, paper and pulp industries. The concentration of phenol in waste waters varies from 10 ppm to 3000 ppm. Phenolic compounds are recognized as toxic carcinogen to human and aquatic life and need to be eliminated (2, 3). The European Union and US Environmental Protection Agency (USEPA) have positioned phenol and its derivatives (e.g. chlorophenols and nitrophenols) on their main concern pollutants list. These phenolic compounds can create an oxygen demand, nasty taste, and whiff, and can wield gloomy effects in ground water resources (4-7).

Careful treatment of waste water containing phenolic compounds is required before its final discharge. Numerous technologies have been investigated for removal of phenol from industrial waste water. They include adsorption, oxidation, and enzymatic treatment. Adsorption appears to be the finest technique to remove phenols (8-12). Most of the physico-chemical methods employed have certain inherent drawbacks such as, tendency to form secondary toxic materials like cyanates, chlorinated phenols, and hydrocarbons. Moreover, the physico-chemical methods of treatment of phenolic wastewater have proven to be costly (13, 14). In spite of successful biological and chemical treatment

techniques, biological method of treatment has turned out to be the most favorable, efficient and prevalent way for phenol removal. Among the four phenol utilizing microbial systems (*Pseudomonas*, *Azotobacter*, *Alcaligenes*, and *Acinetobacter*), *Pseudomonas* has been identified to be effective for eradicating chlorophenol, resorcinol, and other phenolic compound (15, 16). Due to the bacteria's strongest appetite for organic pollutants, it is chosen as a laboratory workhorse. Biological treatment of phenol has attracted great attention due to its environmental friendly approach (17, 18).

Foam separation is still a subject of great attention in mineral processing with a steadily growing number of research studies and industrial application. Biosorptive floatation technique implemented by Zoubollis and Matis for toxic metal removal was extended for phenol separation and worked well (19, 20). Here sorptive phenolics removal has been achieved in the first stage and efficient solid-liquid separation along with unadsorbed traces of phenols in the second stage. The major advantages of biosorptive foam separation of phenol by *Pseudomonas putida* and CTAB is that the phenol concentration in the treated solution was in terms of micrograms which meet out the permitted level. The optimized parameters of biosorption were initialized in foam separation and parameters such as column height, surfactant concentration, and air flow rate were optimized and the residual phenol concentration in the aqueous solution was determined by 4- amino antipyrine method.

Usually, experiments were carried out in such a way that a single factor is examined and analyzed at a time whereas the other variables remain unaltered.

This course of action is called one variable at a time (OVAT). This method is time intensive (the researcher has to screen all variables independently) and requires a large number of experiments. This escalates the cost of study. Additionally, OVAT does not include the communications between the preferred parameters. In order to avoid the limitations of the classical method, statistical experimental design can be used for optimization of process parameters. Response surface methodology (RSM) is an effective statistical technique for designing such experiments, building models and investigating complex processes for the optimization of the target value. Response surface methodology (RSM) was being effective for responses that are influenced by many factors and their interactions. Central composite design (CCD) was used for generation of a response surface analysis model. The statistical implication of the second-order model equation was determined by performing Fisher's statistical tests for analysis of variance (ANOVA). In particular, a good model must be precise and significant based on F-value and p-value in contrast to the lack of fit. Moreover, the proportion of variance exhibited by the correlation coefficient ( $R^2$ ) should be close to 1 as this would demonstrate better correlation between the experimental and predicted values (21-23).

In this present work, the interactions among the following seven operating variables, namely, initial feed (phenol) concentration, pH, biosorbent dosage and time for the biosorption and liquid pool height, surfactant concentration and air flow rate for biosorptive foam separation part was studied using Min Res. V. Statistically optimized condition for maximum removal of phenol from aqueous solution was found. In order to appraise the removal mechanism, equilibrium, and kinetic modeling studies were carried out. Biomass was characterized by FTIR and Zeta potential studies.

## Materials and Methods

### Reagents and analysis

Phenol, Sodium hydroxide flakes (98%), Cetyl Trimethyl Ammonium Bromide (CTAB), Ethanol, and Hydrochloric acid (HCl) were bought from SDFCL (India). Luria-Bertani broth (LB broth), and Nutrient agar were purchased from Hi-media (India). Reagents used in 4-amino antipyrine (4-AAP) procedure for spectrophotometric determination (4-AAP,  $K_3Fe(CN)_6$ ,  $K_2HPO_4$ ,  $KH_2PO_4$  and ammonium hydroxide) were of analytical grade and supplied by Merck (Germany).

Microbial culture, *Pseudomonas putida* (MTCC 1994) was purchased from Microbial Type Culture Collection and Gene Bank and maintained in a standard nutrient agar medium. Inoculum was prepared by suspending grown cells from the slant to the broth. Cells were grown in 250 ml Erlenmeyer flasks containing 100 ml nutrient broth in an incubation shaker (Scigenics Biotech, India). All flasks and media were sterilized and heat inactivated in an autoclave at 121°C, 15 psi for 20 minutes. Biomass was collected by centrifugation and the pellet was washed with 70% ethanol and air dried. Dried biomass was used as an adsorbent.

Sartorius basic meter PB-11 (Germany) was used for measuring pH of feed solution and UV-Vis spectrophotometer Shimadzu-UV-2450 (Japan) used for measuring

the absorbance values of the phenolic solution.

### Stage I: Biosorption experiments

Batch biosorption experiments were carried out in a series of Erlenmeyer flasks, where 100 ml of aqueous phenol (300-700 mg/l), pH (5-9) to be treated was placed in contact with a known mass of biosorbent (0.05-0.25 g in 100 ml) and agitated in an incubation shaker for a time period of (1-3 days) at a fixed speed of 200 rpm and a temperature of 30°C according to experimental design. The samples were filtered through 0.45 µm cellulose acetate membrane filter and analyzed for residual phenol concentration. The interactive effect of various operating parameters such as initial feed concentration, equilibrium time, biosorbent dose, and pH, was studied.

### Stage II: Biosorptive foam separation experiments

Biosorptive foam separation experiments were carried out in a cylindrical glass tube of inner diameter 2 cm with a top hemispherical bend to collect the foam (Fig. 1). A sparger inserted into a close fitting rubber stopper was in turn inserted into the bottom of the glass column. A known volume of phenol-loaded biomass (13.2-46.8 cm) solution from stage I with a predetermined concentration of phenol was taken into the foam column. Surfactant Cetyl trimethyl ammonium bromide (0.132-0.468 w/v %) was added to the bulk solution to stabilize the foam. The air was then admitted through the nozzle into the feed solution at a controlled flow rate (1.16-2.84 lpm). After a time interval of 20 minutes, air supply was bypassed through a two-way valve. The liquid obtained by breaking the foam and the residual pool liquid in the foam column were centrifuged and the supernatant was analyzed to determine the phenol concentration. Concentration of phenol was measured using UV- spectrophotometer at a wavelength of 510 nm from the absorbance calibration curves (24). In the second stage of the biosorptive foam separation, the interactive effect of various operating parameters, namely liquid pool height, surfactant concentration, and air flow rate on percentage removal were studied in detail. Percentage removal was determined by Eq. (1)

$$\text{Removal of phenol (\%)} = \frac{C_o - C_f}{C_o} \times 100 \quad (1)$$

Where;  $C_o$  and  $C_f$  are the phenol concentration (mg/L) in the influent and effluent streams respectively.

## Results and discussion

### Stage I: Biosorption experiments

The experimental ranges and levels along with the

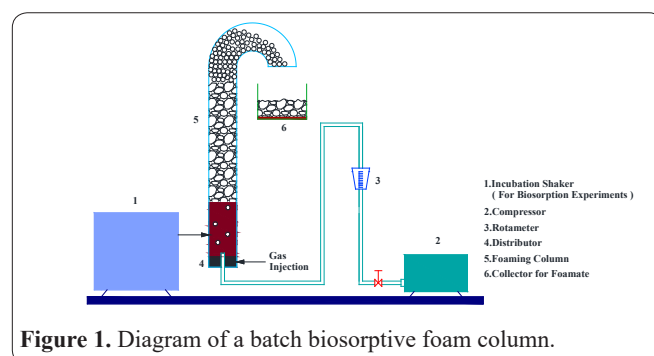


Figure 1. Diagram of a batch biosorptive foam column.

**Table 1.** CCD matrix along with range and its response on percentage removal of phenol from aqueous solution by biosorption using *Pseudomonas putida*.

Runs	Phenol conc. mg/l	pH	Biosorbent dose gm	Time days	Phenol removal %	
					Experimental	Predicted
1	0.00(400)	-2.00(5)	0.00(0.15)	0.00(2.0)	90.71	89.05
2	0.00(400)	0.00(7)	2.00(0.25)	0.00(2.0)	80.57	78.75
3	-2.00(300)	0.00(7)	0.00(0.15)	0.00(2.0)	99.73	94.90
4	0.00(400)	0.00(7)	-2.00(0.05)	0.00(2.0)	91.68	90.38
5	0.00(400)	0.00(7)	0.00(0.15)	0.00(2.0)	98.75	99.04
6	0.00(400)	0.00(7)	0.00(0.15)	0.00(2.0)	99.75	99.04
7	2.00(700)	0.00(7)	0.00(0.15)	0.00(2.0)	87.64	89.36
8	0.00(400)	0.00(7)	0.00(0.15)	2.00(3.0)	82.59	80.27
9	0.00(400)	2.00(8)	0.00(0.15)	0.00(2.0)	86.63	85.17
10	0.00(400)	0.00(7)	0.00(0.15)	-2.00(1.0)	87.64	86.84
11	1.00(500)	-1.00(6)	-1.00(0.10)	-1.00(1.5)	96.73	96.02
12	0.00(400)	0.00(7)	0.00(0.15)	0.00(2.0)	98.75	99.04
13	1.00(500)	-1.00(6)	1.00(0.20)	-1.00(1.5)	87.64	86.81
14	1.00(500)	1.00(8)	-1.00(0.10)	1.00(2.5)	84.61	83.73
15	-1.00(400)	-1.00(6)	1.00(0.20)	1.00(2.5)	87.60	89.30
16	-1.00(400)	1.00(8)	-1.00(0.10)	1.00(2.5)	87.64	90.16
17	-1.00(400)	1.00(8)	-1.00(0.10)	-1.00(1.5)	92.69	93.82
18	1.00(500)	-1.00(6)	1.00(0.20)	1.00(2.5)	83.60	83.90
19	1.00(500)	1.00(8)	1.00(0.20)	1.00(2.5)	80.57	80.58
20	1.00(500)	-1.00(6)	-1.00(0.10)	1.00(2.5)	79.56	80.75
21	-1.00(400)	-1.00(6)	-1.00(0.10)	1.00(2.5)	84.61	85.41
22	0.00(400)	0.00(7)	0.00(0.15)	0.00(2.0)	97.74	99.04
23	1.00(500)	1.00(8)	1.00(0.20)	-1.00(1.5)	77.54	78.17
24	-1.00(400)	1.00(8)	1.00(0.20)	1.00(2.5)	85.62	87.76
25	-1.00(400)	-1.00(6)	1.00(0.20)	-1.00(1.5)	83.60	85.91
26	0.00(400)	0.00(7)	0.00(0.15)	0.00(2.0)	98.75	99.04
27	0.00(400)	0.00(7)	0.00(0.15)	0.00(2.0)	99.76	99.04
28	1.00(500)	1.00(8)	-1.00(0.10)	-1.00(1.5)	93.70	93.69
29	-1.00(400)	1.00(8)	1.00(0.20)	-1.00(1.5)	78.55	79.05
30	-1.00(400)	-1.00(6)	-1.00(0.10)	-1.00(1.5)	92.70	94.38
31	0.00(400)	0.00(7)	0.00(0.15)	0.00(2.0)	99.76	99.04

**Table 2.** ANOVA for response surface quadratic model on percentage removal of phenol from aqueous solution by biosorption using *Pseudomonas putida*.

Source	Sum of Squares	Degrees of freedom	Mean square	F-value	p-value Prob> F
Model	1388.36	14	99.17	20.34	< 0.0001
A-phenol concentration mg/l	46.04	1	46.04	9.44	0.0077
B-pH	22.58	1	22.58	4.63	0.0481
C-biosorbent dose gm	202.65	1	202.65	41.57	< 0.0001
D-time days	64.81	1	64.81	13.3	0.0024
AB	3.15	1	3.15	0.65	0.434
AC	0.56	1	0.56	0.11	0.7405
AD	39.69	1	39.69	8.14	0.0121
BC	39.69	1	39.69	8.14	0.0121
BD	28.25	1	28.25	5.8	0.0294
CD	152.89	1	152.89	31.37	< 0.0001
A <sup>2</sup>	79.06	1	79.06	16.22	0.0011
B <sup>2</sup>	238.93	1	238.93	49.02	< 0.0001
C <sup>2</sup>	353.05	1	353.05	72.43	< 0.0001
D <sup>2</sup>	404.49	1	404.49	82.98	< 0.0001
Residual	73.12	15	4.87		
Lack of Fit	70.25	10	7.02	12.22	0.0064
Pure Error	2.87	5	0.57		
Cor Total	1461.48	29			
Std. Dev.	2.2078			R-Squared	0.9500
Mean	89.2550			Adj R-Squared	0.9033
C.V. %	2.4736			Pred R-Squared	0.7203
PRESS	408.7512			Adeq Precision	13.2877

experimental data obtained from 31 run experiments performed at different combinations of the factors and the predicted data from a response surface analysis were shown in Table. 1. The central point was repeated seven

times. The significance and adequacy of the quadratic model were tested using ANOVA. The results were shown in Table. 2.

The correlation coefficient (R<sup>2</sup>) of the model is

0.9500, which show a good coherence between theoretical and experimental response. The “Predicted R<sup>2</sup>” of 0.7203 is in reasonable agreement with the “Adjusted R<sup>2</sup>” of 0.9033. “Adequate precision” of 13.288 indicates an adequate signal, is a measure of signal to noise ratio. The “Model F-value” of 20.34 implies the model is significant. In this case A, B, C, D, AD, BC, BD, CD, A<sup>2</sup>, B<sup>2</sup>, C<sup>2</sup>, D<sup>2</sup>, are significant model terms. The model established by the regression equation can substitute the experimental real point to explain response results. The regression equation of the process variables is given by Eq. (2).

$$\text{Phenol removal}(Y) = 98.92 - 1.39A - 0.97B - 2.91C - 1.64D - 0.44AB - 0.19AC - 1.58AD - 1.57BC + 1.33BD + 3.09CD - 1.70A^2 - 2.95B^2 - 3.59C^2 - 3.84D^2 \quad (2)$$

Where Y is the phenol removal, A, B, C, and D are phenol concentration in mg/L, pH, and biosorbent dosage in g and time in days.

The above model can be used to predict the biosorption of phenol within the limits of the experimental factors that the actual response values agree well with the predicted response values.

### Interactive effects of process variables on biosorption of phenol

To investigate the significant interactive effects of various process variables on percentage removal of phenol, the three-dimensional profiles of multiple non-linear regression models were shown in Fig.2 (a, b). From the figures, the elliptical shape of contour plot shows significant interaction among the process variables.

The percentage removal of phenol increases when the pH range was increased from the lower level up to a certain limit. After that, the percentage removal decreases. These were due to the fact that the interaction is considered mainly as non-polar, and the forces responsible for adsorption were weak physical. This behavior provides potential for recovery of the adsorbate (phenol) as well as regeneration of adsorbent (*Pseudomonas putida*) by simple nondestructive methods such as ethanol washing (25).

It was observed that the uptake of phenol by *Pseudomonas putida* increased with increase in sorption time up to a certain limit. No significant increase in the sorption was found after two days, and the adsorption was slower. Due to the slower rate of adsorption, a concentration range of 300 mg/L to 700 mg/L was chosen (26). The initial amount of phenol provides an important driving force to overcome all the mass transfer resistances of phenol between the aqueous and solid phase. Accordingly, a high initial concentration would enhance the biosorption process. The increase in sorption capacity with an increase in initial phenol concentration might also due to a higher probability of collision between the phenol molecules and biosorbent (27, 28).

In any adsorption process, the amount of adsorbent plays an important role. In order to evaluate the effect of adsorbent dose (in grams of adsorbent per 100 ml of aqueous phenolic solution) on phenol, experiments were performed with various amounts of *Pseudomonas putida*, ranging from 0.05 to 0.25 g. It is evident from the figures that the biosorbent loading has a profound effect on the percentage removal of phenol. With a fur-

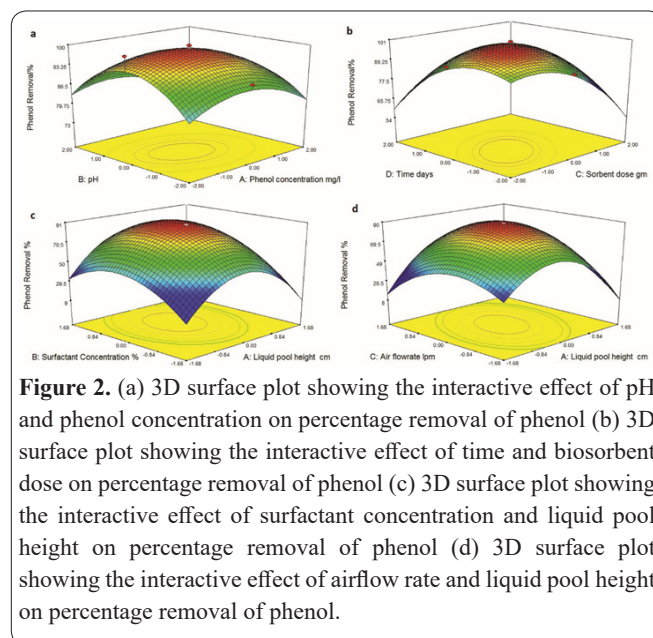


**Figure 2.** (a) 3D surface plot showing the interactive effect of pH and phenol concentration on percentage removal of phenol (b) 3D surface plot showing the interactive effect of time and biosorbent dose on percentage removal of phenol (c) 3D surface plot showing the interactive effect of surfactant concentration and liquid pool height on percentage removal of phenol (d) 3D surface plot showing the interactive effect of airflow rate and liquid pool height on percentage removal of phenol.

ther increase in biosorbent dose over certain limit hadn't allowed any additional improvement. This is because of the binding of almost all the phenol to the sorbent and establishment of equilibrium. Biosorption capacity was high at a low dosages of 0.175 g/100 ml because the biosorption sites remain unsaturated. The decrease in biosorption capacity corresponding to an increase in dose of sorbent above 0.175 g/100 ml is mainly credited to the non-saturation of the biosorption sites. That is, the available phenol molecules are inadequate to cover all the exchangeable sites on the sorbent, resulting in a lower phenol uptake. (29).

### Stage II: Biosorptive foam separation experiments

In the biosorptive foam separation of phenol, the experimental ranges and levels along with the experimental data obtained from 20 run experiments performed at different combinations of the factors and the predicted data from a response surface analysis were shown in Table. 3. The central point was repeated six times. The significance and adequacy of the quadratic model were tested using ANOVA. The results are shown in Table. 4.

The correlation coefficient (R<sup>2</sup>) of the model is 0.9599, which show a good coherence between theoretical and experimental response. The “Predicted R<sup>2</sup>” of 0.7976 is in reasonable agreement with the “Adjusted R<sup>2</sup>” of 0.9238. “Adequate precision” of 15.176 indicates an adequate signal, is a measure of signal to noise ratio. The “Model F-value” of 26.58 implies the model is significant. Values of “Probability F” less than 0.0500 indicates model terms are significant. In this case B, AC, A<sup>2</sup>, B<sup>2</sup>, C<sup>2</sup> are significant model terms. The model established by the regression equation can substitute the experimental real point to explain response results. The second order regression equation of the process variables is given by Eq. (3).

$$\text{Phenol removal}(Y) = 89.22 - 0.65A + 6.11B + 0.99C + 1.13AB + 4.69AC - 4.87BC - 14.05A^2 - 9.05B^2 - 8.78C^2 \quad (3)$$

Where Y is the phenol removal, A, B and C is liquid pool height, surfactant concentration, and airflow rate respectively. The p-value less than 0.05 indicate model terms are significant. The values greater than 0.05,

**Table 3.** CCD matrix along with range and its response on percentage removal of phenol from aqueous solution by biosorptive foam separation using *Pseudomonas putida* and CTAB.

Run	liquid pool height cm	Surfactant w/v %	Air flow rate Lpm	Percentage removal (%)	
				Experimental	Predicted
1	0.00(30)	0.00(0.30)	1.68(2.84)	70.00	66.04
2	0.00(30)	0.00(0.30)	-1.68(1.16)	68.00	62.72
3	0.00(30)	0.00(0.30)	0.00(2.00)	88.89	89.22
4	-1.00(20)	-1.00(0.20)	-1.00(1.50)	48.45	51.84
5	1.00(40)	-1.00(0.20)	1.00(2.50)	57.00	59.99
6	0.00(30)	0.00(0.30)	0.00(2.00)	88.89	89.22
7	1.00(40)	1.00(0.40)	1.00(2.50)	61.59	64.73
8	0.00(30)	0.00(0.30)	0.00(2.00)	88.38	89.22
9	-1.00(20)	-1.00(0.20)	1.00(2.50)	52.00	54.18
10	-1.00(20)	1.00(0.40)	-1.00(1.50)	68.00	71.54
11	0.00(30)	0.00(0.30)	0.00(2.00)	89.34	89.22
12	1.00(40)	1.00(0.40)	-1.00(1.50)	58.77	63.12
13	0.00(30)	-1.68(0.132)	0.00(2.00)	57.00	53.34
14	1.68(46.80)	0.00(0.30)	0.00(2.00)	53.20	48.39
15	0.00(30)	1.68(0.468)	0.00(2.00)	79.47	73.90
16	1.00(40)	-1.00(0.20)	-1.00(1.50)	36.00	38.90
17	-1.00(20)	1.00(0.40)	1.00(2.50)	50.76	54.40
18	0.00(30)	0.00(0.30)	0.00(2.00)	88.89	89.22
19	-1.68(13.2)	0.00(0.30)	0.00(2.00)	55.00	50.57
20	0.00(30)	0.00(0.30)	0.00(2.00)	89.34	89.22

**Table 4.** ANOVA for response surface quadratic model on percentage removal of phenol from aqueous solution by biosorptive foam separation using *Pseudomonas putida* and CTAB in coded levels

Source	Sum of Squares	Degrees of freedom	Mean Square	F value	p-value Prob> F
Model	5260.59	9	584.51	26.58	< 0.0001
A-height cm	5.77	1	5.77	0.26	0.6195
B-surfactant conc. w/v%	510.08	1	510.08	23.20	0.0007
C-air flow rate lpm	13.34	1	13.34	0.61	0.4541
AB	10.23	1	10.23	0.47	0.5106
AC	175.85	1	175.85	8.00	0.0179
BC	189.83	1	189.83	8.63	0.0148
A <sup>2</sup>	2844.57	1	2844.57	129.36	< 0.0001
B <sup>2</sup>	1180.73	1	1180.73	53.69	< 0.0001
C <sup>2</sup>	1111.22	1	1111.22	50.53	< 0.0001
Residual	219.90	10	21.99		
Lack of Fit	219.26	5	43.85	343.21	< 0.0001
Pure Error	0.64	5	0.13		
Cor Total	5480.48	19			
Std. Dev.	4.6893		R-Squared		0.9599
Mean	67.4484		Adj R-Squared		0.9238
C.V. %	6.9525		Pred R-Squared		0.7976
PRESS	1657.2231		Adeq Precision		15.1764

indicates that the model terms are not significant. This model can be used to predict the biosorption of phenol as actual response values agree well with the predicted response values.

### Interactive effects of liquid pool height, surfactant concentration, and air flow rate on biosorptive foam separation of phenol

In order to investigate the effects of various process variables on percentage removal of phenol, the response surface curves and contour plots from the interactions between the variables were shown in three-dimensional profiles of multiple nonlinear regression models Fig. 2 (c, d)

From the figures, it is observed that as the height of the liquid pool increased from a lower level up to a certain point, the amount of phenol removed to the foam also increases. This is due to the fact that as the height

increases the residence time of the bubbles in the liquid pool increases. After a certain point, the adsorption of phenol onto bubbles could reach equilibrium, beyond which the percentage removal decreases (19).

As the surfactant CTAB concentration increases percentage removal too increases and this is because aqueous phenol is slightly acidic and cationic surfactant attracts anionic phenolate and hence an increased surface activity too. Subsequently, as the surface is saturated, further increase in CTAB concentration significantly slow down the rate of drainage of the foam and surplus surfactant can form micelles. Therefore, the phenol percentage removal reduced with an increase in the surfactant concentration after a certain level (30).

Initially, as the airflow rate is increased from lower level to higher, percentage removal also increases. This is due to the fact that, initially at low flow rates, the bubble sizes are larger and therefore at lower rates

bubbles agglomerates and becomes larger in size and coalesces resulting in more drainage of phenol. However, with further increase in airflow rate above a certain point, the percentage removal decreases which is due to the fact that the foam bubble size decreased and coalescence and drainage decreased (31,32).

**Isotherm studies**

The biosorption experiments were performed by isothermal batch mode at 30°C. The amount adsorbed at equilibrium  $q_e$  is calculated by the Eq. (4)

$$q_e = \frac{(C_0 - C_e)V}{m} \tag{4}$$

Where  $C_0$  is the initial phenol concentration (mg/l),  $V$  is the volume of solution (L) and  $m$  is the dry weight of the biosorbent (g). Equilibrium data were fitted using seven different isotherm models, namely Langmuir, Freundlich, Tempkin, Redlich-Peterson, BET, Dubinin Radushkevich and Elovich isotherm models (33-38).

Results showed that Langmuir isotherms fitted the data well with the later best with an  $R^2$  value of 0.9544 and were explained and shown in Fig. 3.

The Langmuir isotherm model is defined by Eq. (5) and the linear form of the isotherm is given by Eq. (6)

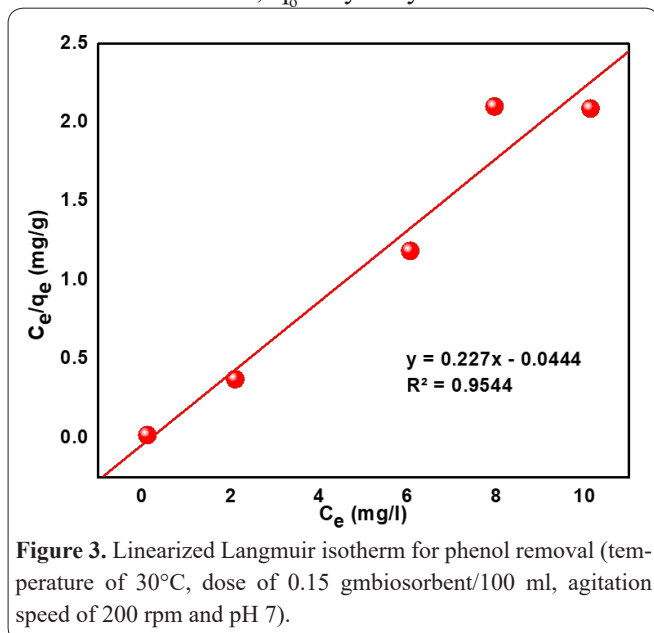
$$q_e = \frac{q_0 K_L C_e}{1 + K_L C_e} \tag{5}$$

$$\frac{C_e}{q_e} = \frac{1}{K_L q_0} + \frac{C_e}{q_0} \tag{6}$$

Where;  $q_0$ : Empirical Langmuir constant which represents the maximum adsorption capacity (mg/g),  $K_L$ : Constant related to the energy of adsorption (L/mg).

The plot of  $\frac{C_e}{q_e}$  vs  $C_e$  yields a straight line with slope  $\frac{1}{q_0}$  and intercept  $\frac{1}{K_L q_0}$

The values of  $q_0$  and  $K_L$  can be calculated from the slope and intercept of the linear curve. The  $q_0$  value represents the total number of surface sites per mass of adsorbent. In an ideal case,  $q_0$  would be equal for all adsorbates. However,  $q_0$  may vary somewhat between



different compounds because of differences in adsorbate sizes. The constant  $K_L$  is defined as the equilibrium constant of the adsorption reaction.

**Biosorption kinetics**

Biosorption kinetics was studied at 30°C and the rate was monitored and the results were compared with theoretical models. Adsorbed amount of phenol at any time  $q_t$  is calculated by Eq. (7)

$$q_t = \frac{(C_0 - C_t)V}{m} \tag{7}$$

Where  $q_t$  is the amount of biosorption at time  $t$  (mg/g),  $C_0$  is the initial concentration of the phenolic compound in the solution (mg/L),  $C_t$  is the concentration of the phenolic compound in the solution at time  $t$  (mg/L),  $V$  is the volume of solution (L) and  $m$  is the mass of the biosorbent (g).

Pseudo first order, Pseudo second order, Elovich, Intraparticle diffusion, Mass transfer diffusion and Bangham kinetic models were tested in this study (39-42). Results showed that the Bangham kinetic model fitted the data well and shown in Fig. 4.

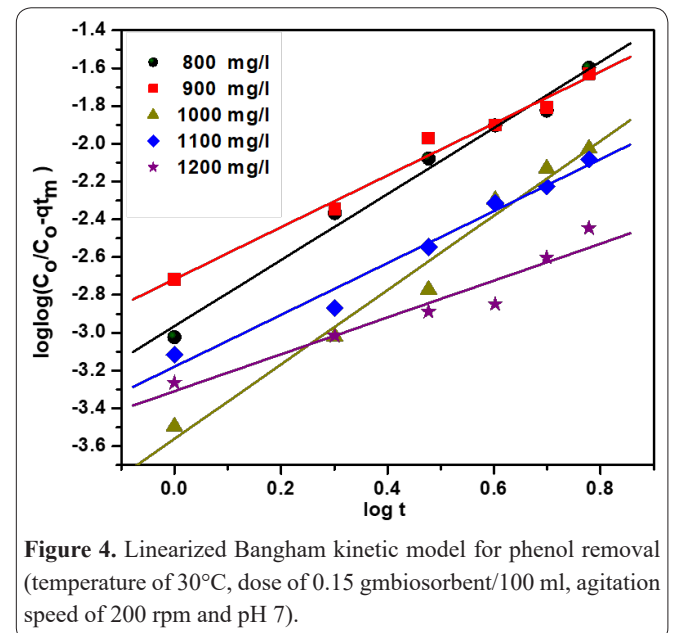
The Bangham kinetic model is a double logarithmic plot implying the participation of the diffusion processes in the rate determining step. Therefore, the rate determining step may be controlled by film or pore diffusion or a mixture of both. The Bangham's model is given by Eq. (8)

$$\log \log \frac{C_0}{C_0 - q_t m} = \frac{\log k_0 m}{2.303 v} + \alpha \log t \tag{8}$$

Where;  $C_0$  is the initial concentration of adsorbate in solution mg/L,  $V$  is the volume of solution (L) and  $m$  is the mass of the biosorbent (g),  $q_t$  is the amount of sorbate retained at a time  $t$  (mg/g),  $\alpha$  and  $K_0$  are constants.

**Fourier transform infrared (FTIR) analysis**

FTIR spectroscopy method was used to obtain information on the functional groups and hence sorption mechanism. The FTIR spectra of the biosorbent were recorded on a Perkin-Elmer spectrum version



10.03.09, instrument model spectrum two and instrument serial number 92626. FTIR spectra over a range of 4000–400  $\text{cm}^{-1}$ , for biosorbent as fresh feed, after biosorption of phenol and after biosorptive foam separation were shown in Fig. 5. Chemical characteristics of the samples were analyzed by FTIR spectrometry after the samples were prepared as KBr discs. FTIR spectrum of the fresh biosorbent exhibited broad absorption bands around 3600–3000  $\text{cm}^{-1}$  indicating the presence of –OH stretching vibrations. The band at 2927  $\text{cm}^{-1}$  indicates C–H group. The peak at 1631.32  $\text{cm}^{-1}$  can be designated as the C=O stretching in carboxyl or amine groups. The peak at 1477.16  $\text{cm}^{-1}$  can be designated as the C–H bending. The peak at 1384.38  $\text{cm}^{-1}$  is indicative of methyl symmetrical C–H bending group. The peak at 1354.03  $\text{cm}^{-1}$  can be designated as aromatic P=O stretching. The peak at 1242.31  $\text{cm}^{-1}$  can be designated as aliphatic P=O stretching. The peak at 1076.06  $\text{cm}^{-1}$  can be indicative of the  $\text{NH}_3^+$  rocking vibrations. The peak at 765.76  $\text{cm}^{-1}$  can be indicative of the  $\text{NH}_2$  wagging and twisting vibrations. The peak at 699.96  $\text{cm}^{-1}$  can be indicative of the C–H stretching vibrations. The FTIR spectrum of the phenol treated biosorbent exhibited broad absorption bands around 3600–3000  $\text{cm}^{-1}$  indicating the presence of –OH stretching vibrations. The band at 3291.46  $\text{cm}^{-1}$  indicates =C–H stretching group.

The peak at 2927.63  $\text{cm}^{-1}$  can be designated as the C–H stretching in carboxyl or amine groups. The peak at 1601.56  $\text{cm}^{-1}$  can be designated as the C=O stretching in carboxyl or amine groups. The peak at 1446.17  $\text{cm}^{-1}$  can be designated as the C–H bending. The peak at 1384.16  $\text{cm}^{-1}$  is indicative of methyl symmetrical C–H bending group. The peak at 1242.84  $\text{cm}^{-1}$  can be designated as aliphatic P=O stretching. The peak at 1076.19  $\text{cm}^{-1}$  can be indicative of the  $\text{NH}_3^+$  rocking vibrations. The peak at 764.70  $\text{cm}^{-1}$  can be indicative of the  $\text{NH}_2$  wagging and twisting vibrations. The peak at 698.76  $\text{cm}^{-1}$  can be indicative of the C–H stretching vibrations. The phenol CTAB treated bacteria showed a broad peak around 3600–3000  $\text{cm}^{-1}$ , which could be attributed to sorption of phenol onto bacteria. The band at 3424.74  $\text{cm}^{-1}$  is indicative of the O–H stretching region. The peak at 2921.13  $\text{cm}^{-1}$  can be designated as the C–H stretching in carboxyl or amine groups. The peak at 2852.16  $\text{cm}^{-1}$

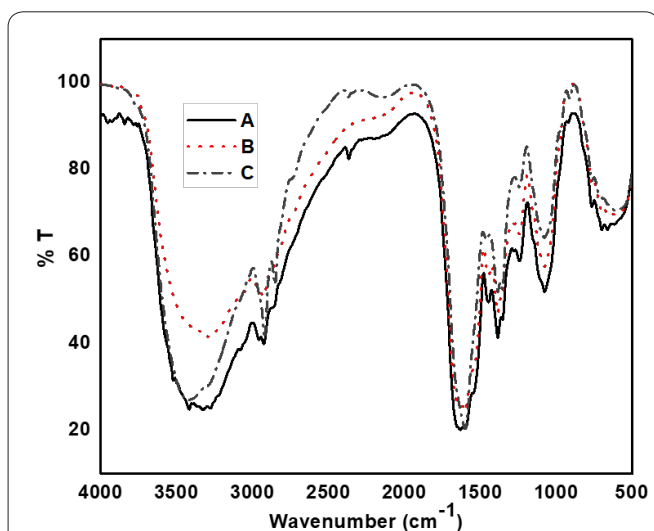


**Figure 5.** FTIR spectrum of (A) Fresh biosorbent, (B) Phenol loaded, and (C) Phenol CTAB loaded Biomass.

can be designated as the  $\text{CH}_2$  symmetric stretching. The peak at 2368.79  $\text{cm}^{-1}$  designates C–H stretching. The peak at 2151.51  $\text{cm}^{-1}$  can be designated as the combination N–H and O–H stretching. The peak at 1599.56  $\text{cm}^{-1}$  can be designated as the C=O stretching in carboxyl or amine groups. The peak at 1460.67  $\text{cm}^{-1}$  can be designated as the C–H bending. The peak at 1384.86  $\text{cm}^{-1}$  is indicative of methyl symmetrical C–H bending group. The peak at 1355.39  $\text{cm}^{-1}$  is indicative of C–H bending bands. The peak at 1243.08  $\text{cm}^{-1}$  can be designated as aliphatic P=O stretching. The peak at 1077.60  $\text{cm}^{-1}$  can be indicative of the  $\text{NH}_3^+$  rocking vibrations. The peak at 911.92  $\text{cm}^{-1}$  can be indicative of C–H out of plane bending bands. The peak at 764.69  $\text{cm}^{-1}$  can be indicative of the  $\text{NH}_2$  wagging and twisting vibrations. The peak at 612.89  $\text{cm}^{-1}$  can be indicative of the C–H out of plane bending bands (43).

### Electrokinetic studies

The zeta ( $\zeta$ ) potential measurements of the *Pseudomonas putida* cells were performed as a function of pH, fresh the initial stage and after biosorptive foam separation using the micro electrophoretic apparatus Zeta Plus (Brookhaven Instruments Corporation, USA). The electrophoretic mobility determined was converted to  $\zeta$  potential using the Smoluchowski approximation. The reported values are an average of 10 measurements.

The  $\zeta$  potential measurements provide information regarding the surface charge of fresh and phenol CTAB loaded cells. Fig. 6 depicts  $\zeta$  potential of fresh and phenol CTAB loaded cells at different pH values, adjusted with the addition of 0.1M NaOH and HCl. The electrokinetic study provides preliminary information regarding the type of surfactant to be added for the separation of fine particles by flotation, and possible biosorption mechanism. The fact that the observed negative charge throughout the pH range examined, showing an isoelectric point (IEP) at a pH of around 3, proved the application of the cationic surfactant, renders hydrophobicity and hence, floatability. The presence of various carbohydrate related moieties and functional groups like carboxyl, amide, phosphate, and hydroxyl, provide a net surface charge to the cell wall. The dissociation of these functional groups seems to be a general phenomenon. The observation of an isoelectric point (IEP) at a pH of around 3, is in agreement with the fact that most of the bacterial cells have an isoelectric point at a pH value of less than 4 and, reflects mixed contributions of protein or peptidoglycan-associated  $\text{COOH}^-$  or  $\text{NH}_3^+$  and may result from a combination of  $\text{NH}_3^+$  containing polymers and low pKa anionic polysaccharides containing phosphate or carboxyl groups. No significant change is observed on the surface charge of the non-living biomass when examined alone or in the presence of cationic surfactant. The phenol binding properties of Gram-negative bacteria are largely due to positively charged amino groups, which are part of the cell wall structure. Due to this fixed cation content, they exhibit high sorption capacities. From the above discussions, it is clear that the zeta-potential changes according to changes in the solution. The zeta-potential measurements make it possible to follow the changes that take place in the solution. After biosorptive foam separation, the zeta potential of the biomass becomes less negative. This could

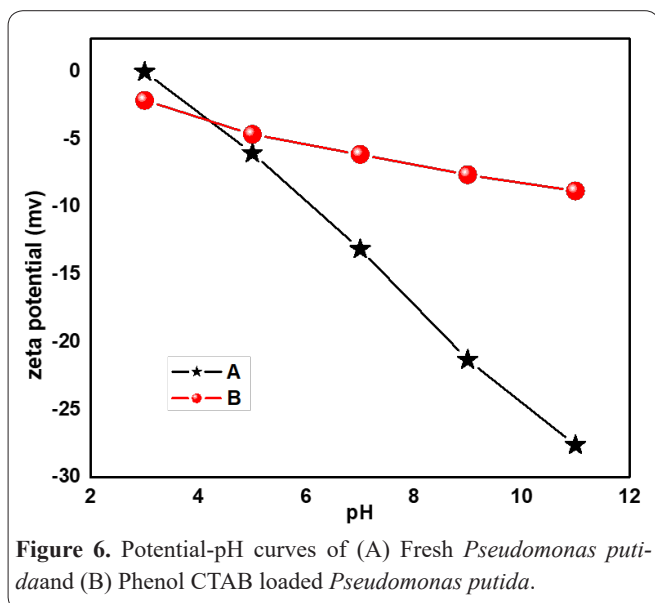


**Figure 6.** Potential-pH curves of (A) Fresh *Pseudomonas putida* and (B) Phenol CTAB loaded *Pseudomonas putida*.

be attributed to the electrostatic interaction between the biomass, CTAB and phenolate ions. This effect is caused by the dissociation of the functional groups at high pH values, which will promote an electrostatic attraction toward negatively charged phenolate ions in the solution (44-47).

## Conclusions

The outcomes of biosorptive foam separation of phenolic compounds by *Pseudomonas putida* and cationic surfactant has proved to be a most promising technique. It is a two stage process where sorption of phenol over the dead cells constitutes the first stage and separation of phenol loaded biomass, and a clear underflow constitutes the next. "Min Res V" was successfully employed and the ANOVA showed a high coefficient of determination value ( $R^2=0.9500$ ) for biosorption experiments and ( $R^2=0.9599$ ) for biosorptive foam separation experiments, thus ensuring a satisfactory adjustment of the second order regression model with the experimental data. Reasonable predicted equations were obtained for the removal of phenol using RSM to optimize the parameters. A maximum predicted value of percentage removal of phenol is 99.95% and the conditions for maximum phenol removal are 575 mg/L of initial phenol concentration, a pH of 7.1, 0.175 g of dry bacterial cells, and 2 days of time period, and the conditions for the second stage of biosorptive foam separation are a liquid pool height of 24 cm, cationic surfactant concentration of 0.15% (w/v), and an air flow rate of 2 Lpm. Isotherm and kinetic studies reveal that the biosorption process followed Langmuir isotherm model ( $R^2=0.9544$ ) and Bangham kinetic model ( $R^2=0.9857$ ). FTIR spectra for fresh biosorbent, after biosorption, and after biosorptive foam separation were generated to indicate their interactions and bonding. The zeta potential of the bacteria was affected by the presence of phenol at different pH values, showing isoelectric point at a pH of around 3. The results obtained from this study showed that *Pseudomonas putida* can be a good sorbent for the removal of phenol from an aqueous solution and CTAB can be a most appropriate surfactant. The recovery of phenol loaded biomass and final traces of phenol by floatation were found to be of the order of 99.95%.

## Acknowledgements

The authors express their gratitude for the financial support extended by the Department of Science and Technology (DST-Government of India). Grant. No: SR/FT/ETA-0017/2012 and Technical Education Quality Improvement program (TEQIP II).

## References

- Annadurai G, Juang R S, Lee DJ. Biodegradation and adsorption of phenol using activated carbon immobilized with *Pseudomonas putida*, *J Environ Sci Heal A* 2002; 37: 1133–1146.
- Ahmaruzzaman M, Sharma DK. Adsorption of phenols from wastewater. *J Colloid Interf Sci.* 2005; 287: 14-24.
- Jiang Y, Jianping W, Bai J, Jia X, Hu Z. Biodegradation of phenol at high initial concentration by *Alcaligenes faecalis*. *J Hazard Mater* 2007; 12: 321-328.
- Annadurai G, Babu SR, Mahesh KPO, Murugesan I. Adsorption and bio-degradation of phenol by chitosan-immobilized *Pseudomonas putida* (NICM 2174). *Bioprocess Eng* 2000;2: 493-501.
- Dabrowski, A, Podkoscielny P, Hubicki T, Barczak M. Adsorption of phenolic compounds by activated carbon – a critical review. *Chemosphere.* 2005; 58: 1049–1070.
- Lu Q, Sorial GA. The effect of functional groups on oligomerization of phenolics on activated carbon. *J Hazard Mater* 2007; 148: 436–445.
- Hamdaoui O, Naffrechoux E, Modelling of adsorption isotherms of phenol and chlorophenols onto granular activated carbon Part II: Models with more than two parameters. *J Hazard Mater* 2007;147: 401–411.
- Álvarez PM, García-Araya JF, Beltrán, FJ, Masa FJ, Medina F. Ozonation of activated carbons: effect on the adsorption of selected phenolic compounds from aqueous solutions. *J Colloid Interf Sci.* 2005; 283: 503–512.
- Pan B, Zhang W, Zhang Q, Zheng S. Adsorptive removal of phenol from aqueous phase by using a porous acrylic ester polymer, *J. Hazard. Mater* 2008; 157: 293–299.
- Carmona de Luca A, Valverde JL, Velasco B, Rodríguez JF. Combined adsorption and ion exchange equilibrium of phenol on Amberlite IRA-420 *Chem Eng J* 2006;117:155–160.
- Mao X, Buchanan ID, Stanley SJ. Phenol removal from aqueous solution by fungal peroxidase *J Environ Eng Sci.* 2006;5: 103–109.
- Sobecka S, Tomas BM, Morawski, AW. Removal of micro pollutants from water by ozonisation bio filtration process *Desalination.* 2005; 182: 151–157.
- Sakurai A, Masuda M, Sakakibara M. Effect of surfactants on phenol removal by the method polymerization and precipitation catalyzed by *Coprinus cinereus* peroxidase *J Chem Technol. Biotechnol.* 2003; 78: 952–958.
- Bandyopadhyay K, Das D, Maiti BR. Kinetics of phenol degradation using *Pseudomonas putida* MTCC 1194, *Bioprocess Eng,* 1998; 18: 373-377
- Hill GA, Robinson CW. Substrate inhibition kinetics: phenol degradation by *Pseudomonas putida* *Biotechnol Bioeng* 1975; 40: 1353±1358.
- Sivasubramanian, Namasivayam SKR, Optimization of parameters for phenol degradation using immobilized *Candida tropicalis* SSK01 in batch reactor *J Environ Biol.* 2014; 35:531-536.
- Yang CF, Lee CM. Enrichment, isolation, and characterization of phenol-degrading *Pseudomonas resinovorans* strain P-1 and *Brevibacillus* sp. Strain P-6, *Int. Biodeterior Biodegrad.* 2007; 59: 206-210.
- Wei G, Yu J, Zhu Y, Chen W, Wang L. Characterization of phenol degradation by *Rhizobium* sp. CCNWTB 701 isolated from

Astragalus chrysopteruin mining tailing region J Hazard Mater. 2007;22: 85-91.

19. Arulmozhi M, Begum KMMS, Anantharaman N. Continuous foam separation of heavy metal ions from electroplating industrial effluent Chem Eng Commun 2011; 198: 541 -551.

20. Zouboulis AI, Matis KA. Biosorptive flotation for metal ions removal: the influence of surface tension Desalination. 2009; 248: 740–752.

21. Saravani N, Arulmozhi.M. Influence of various process parameters on the biosorptive foam separation performance of o-cresol onto Bacillus cereus and CetylTrimethyl Ammonium Bromide, J Taiwan Inst Chem. Eng. 2016; 67: 263–270.

22. Mandal S, Bhunia B, Kumar A, Dasgupta D MandalT, DattaS. and Bhattacharya. PA. Statistical approach for optimization of media components for phenol degradation by Alcaligenes faecalis using Plackett–Burman and response surface methodology, Desalin and Water Treat., 2013; 51: 6058–6069.

23. Li J, Liang L, Borrer CM, Cook CA, Montgomery DC. Graphical Summaries to Compare Prediction Variance Performance for Variations of the Central Composite Design for 6 to 10 Factors, Qual Technol Qual Manage2009; 6: 433-449.

24. Agarry SE, Solomon BO and Layokun.SK. Optimization of process variables for the microbial degradation of phenol by Pseudomonas aeruginosa using response surface methodology Afr.J Biot 2008; 7: 2409-2416.

25. Nadavala SK. Biosorption of phenol and o-chlorophenol from aqueous solutions on to chitosan–calcium alginate blended beads J Hazard Mater. 2009;162: 482–489.

26. Kumar A, Kumar S, Kumar S, Biodegradation kinetics of phenol and catechol using Pseudomonas putida MTCC 1194 Biochem. Eng J. 2005;22: 151–159.

27. Abdullah MAM. The potential of different bio adsorbents for removing phenol from its aqueous solution Environ Monit Assess 2013;185: 6495–6503.

28. Wu J, Yu HQ. Biosorption of 2, 4-dichlorophenol from aqueous solution by Phanerochaete chrysosporium biomass: Isotherms, kinetics and thermodynamicsJ Hazard Mater. 2006; 137:498–508.

29. Kumar NS, Min K. Phenolic compounds bio sorption onto Schizophyllum commune fungus: FTIR analysis, kinetics and adsorption isotherms modeling Chem Eng J 2011; 168: 562–571.

30. Arulmozhi M, Begum KM M S, Anantharaman N. Continuous foam fractionation of chromium (VI) ions from aqueous and industrial effluents, Desalin and Water Treat. 2013; 1-11.

31. Wong CH, Hussain MM and Davies CE, Performance of a continuous foam separation column as a function of process variables. Biopro Biosyst Eng 2001; 24: 73-81.

32. Qu YH, Zeng GM, Huang JH, Xu K, Fang YY, Li X, Liu HL. Recovery of surfactant SDS and Cd<sup>2+</sup> from permeate in MEUF using a continuous foam fractionator, J Hazard Mater. 2008; 155:32-38.

33. Li JM, Meng XG, Hu CW, Du J. Adsorption of phenol, p-chlorophenol and p-nitrophenol onto functional chitosan. Bioresour-Technol. 2009; 100:1168–1173.

34. Saravani N, Arulmozhi M, Vaidhegi K, Experimental Investigation on Adsorption of Phenol onto Micrococcus lylae and CetylTrimethyl Ammonium Bromide, Clean (Weinh) 2016; 44: 1489–1498.

35. Feng-Chin W, Bing-Lan L, Keng-Tung W, Ru-Ling T. A new linear form analysis of Redlich–Peterson isotherm equation for the adsorptions of dyes Chem Eng Journal 2010;162: 21–27.

36. Ofomaja AE, Unuabonah EI, Adsorption kinetics of 4-nitrophenol onto a cellulosic material, mansonia wood sawdust and multistage batch adsorption process optimization Carbohydr Polym, 2011;83:1192–1200

37. Dang VBH, Doan HD, Vu TD. Lohi A. Equilibrium and kinetics of biosorption of cadmium (II) and copper (II) ions by wheat straw BioresourceTechnol,2009 ;100 :211–219

38. Hamdaoui O, Naffrechoux E. Modeling of adsorption isotherms of phenol and chlorophenols onto granular activated carbon Part I. Two-parameter models and equations allowing determination of thermodynamic parameters J Hazard Mater 2007;147 :381–394

39. Abramian L, Rassy H.E. Adsorption kinetics and thermodynamics of azo-dye Orange II onto highly porous Titania aerogel. Chem Eng Journal, 2009; 150:403–410

40. Kumar NS, Woo HS, Min K, Equilibrium and kinetic studies on biosorption of 2,4,6-trichlorophenol from aqueous solutions by Acacia leucocephala bark. Colloid Surface B 2012; 94: 125– 132

41. Hameed BH, Mahmoud DK, Ahmad AL. Equilibrium modeling and kinetic studies on the adsorption of basic dye by a low-cost adsorbent: Coconut (Cocos nucifera) bunch waste J Hazard Mater, 2008; 158:65–72.

42. Ofomaja AE, Unuabonah EI. Adsorption kinetics of 4-nitrophenol onto a cellulosic material, mansonia wood sawdust and multistage batch adsorption process optimization Carbohydr Polym. 2011; 83:1192–1200

43. Stuart B. Infrared spectroscopy fundamentals and applications, John Wiley and sons

44. Nazari AM, Cox PW, Waters KE. Biosorptive flotation of copper ions from dilute solution using BSA-coated bubbles, Miner Eng 2015; 75:140-145.

45. Peleka EN, Matis KA. Bioremoval of Metal Ion and Water Treatment in a Hybrid Unit, Sep. Sci. Technol. 2009; 44: 3597–3614.

46. Hua Z, Yongbing J, Guangming Z, Zhifeng L, Liuxia L, Yang L, Xin Y, Mingyong L, Yibin H. Effect of low-concentration rhamnolipid on adsorption of Pseudomonas aeruginosa ATCC 9027 on hydrophilic and hydrophobic surfaces J Hazard Mater. 2015; 285: 383–388

47. Ana Elisa CB, Mauri'cio Leonardo T, Luciana Maria S. de Mesquita, Surface chemistry fundamentals of biosorption of Rhodococcus opacus and its effect in calcite and magnesite flotation, Miner Eng 2008; 21: 83–92.